CCD PHOTOMETRY OF 29 ASTEROIDS AT SOPOT ASTRONOMICAL OBSERVATORY: 2020 JULY-2021 SEPTEMBER

Vladimir Benishek
Belgrade Astronomical Observatory
Volgina 7, 11060 Belgrade 38, SERBIA
vlaben@yahoo.com

(Received: 2021 October 15)

Lightcurves and synodic rotation periods for 29 asteroids determined from CCD photometric data obtained at Sopot Astronomical Observatory (SAO) over the time span 2020 July - 2021 September are presented in this paper.

Photometric observations of 29 asteroids were conducted at Sopot Astronomical Observatory (SAO) from 2020 July through 2021 September in order to determine the asteroids' synodic rotation periods. For this purpose, two 0.35-m *f*/6.3 Meade LX200GPS Schmidt-Cassegrain telescopes were employed. The telescopes are equipped with a SBIG ST-8 XME and a SBIG ST-10 XME CCD cameras. The exposures were unfiltered and unguided for all targets. Both cameras were operated in 2×2 binning mode, which produces image scales of 1.66 arcsec/pixel and 1.25 arcsec/pixel for ST-8 XME and ST-10 XME cameras, respectively. Prior to measurements, all images were corrected using dark and flat field frames.

Photometric reduction was conducted using *MPO Canopus* (Warner, 2018a). Differential photometry with up to five comparison stars of near solar color ($0.5 \leq B\text{-}V \leq 0.9$) was performed using the Comparison Star Selector (CSS) utility. This helped ensure a satisfactory quality level of night-to-night zero-point calibrations and correlation of the measurements within the standard magnitude framework. Field comparison stars were calibrated using standard Cousins R magnitudes derived from the Carlsberg Meridian Catalog 15 (VizieR, 2021) Sloan r' magnitudes using the formula: $R = r' - 0.22$ in all cases presented in this paper. In some instances, small zero-point adjustments were necessary in order to achieve the best match between individual data sets in terms of achieving the most favorable statistical indicators of Fourier fit goodness.

Lightcurve construction and period analysis was performed using *Perfindia* custom-made software developed in the R statistical programming language (R Core Team, 2020) by the author of this paper. The essence of its algorithm is reflected in finding the most favorable solution for rotational period by minimizing the *residual standard error* of the lightcurve Fourier fit.

The lightcurve plots presented in this paper show so-called 2% error for rotational periods, i.e., an error that would cause the last data point in a combined data set by date order to be shifted by 2% (Warner, 2012) and represented by the following formula: $\Delta P = (0.02 \cdot P^2) / T$, where P and T are the rotational period and the total time span of observations, respectively. Both of these quantities must be expressed in the same units.

Some of the targets presented in this paper were observed within the Photometric Survey for Asynchronous Binary Asteroids (*BinAstPhot Survey*) under the leadership of Dr Petr Pravec from Ondřejov Observatory, Czech Republic.

Table I gives the observing circumstances and results.

Observations and results

428 Monachia. Several previously determined synodic rotation periods (for example, Wisniewski et al. (3.63384 h, 1997), Warner (3.633 h, 2014), Behrend (3.6335 h, 2016web), a sidereal period by Durech et al. (3.63360 h, 2020), Pal et al. (3.6343 h, 2020)) are very well consistent with a value of P = 3.365 ± 0.003 h found from SAO data obtained over four nights in 2021 March.

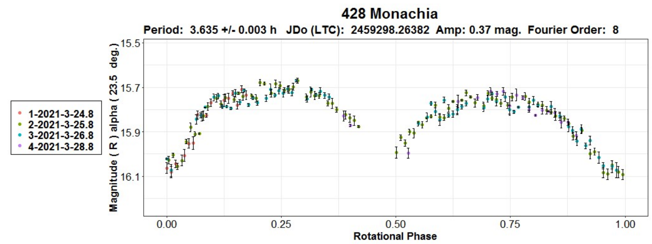

878 Mildred. Stephens and French (2011) found a rotation period of 2.660 h. Period (P = 2.6607 ± 0.0003 h) found from the data obtained at SAO on five nights in 2021 August-September is in full agreement with the previously reported result.

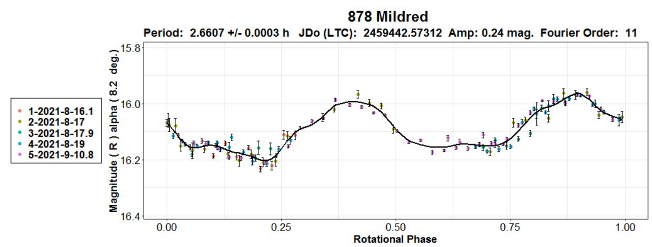

894 Erda. Although the rotational cycle corresponding to the found period value of P = 4.700 ± 0.009 h is not fully covered by the data obtained on three consecutive nights in 2021 August, the established period result fits quite well into the previously determined values by Behrend (4.69 h, 2001web), Stephens (4.69 h, 2002) and Higgins and Goncalves (4.6897, 2007).

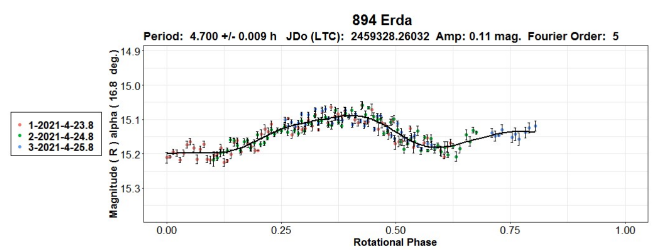

1129 Neujmina. Data from three consecutive nights in 2021 April resulted in a period of P = 5.06 ± 0.02 h. Carbo et al. (2009) and Ditteon and West (2011) previously found values of 5.089 h and 5.0844 h, respectively.

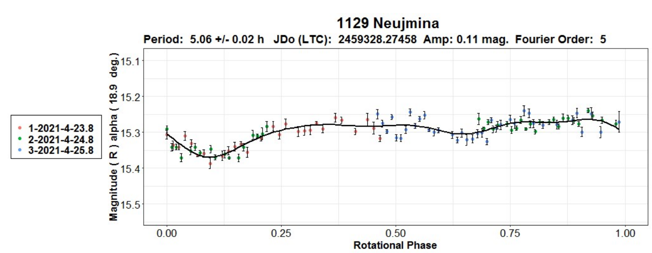

1322 Coppernicus. Several period results have been reported previously of which only two of them determined more recently by Fauerbach and Brown (4.354 h, 2018) and Noschese et al. (4.354 h, 2018) are completely consistent with each other. A period of P = 4.352 ± 0.003 h derived from the late 2021 June SAO data is in very good agreement with the stated recent results.

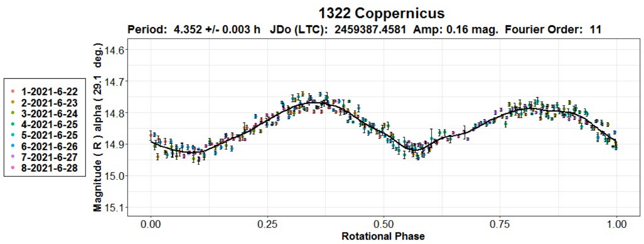

1671 Chaika. Two previously reported rotation period results by Behrend (3.7718 h, 2005web) and Menke et al. (3.774 h, 2008) are statistically identical with a period value of P = 3.771 ± 0.004 h obtained from the SAO data collected on four consecutive nights in 2021 June.

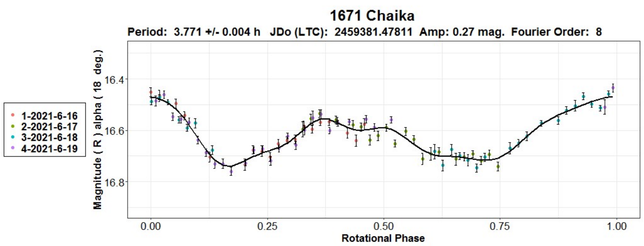

1713 Bancilhon. No reports on rotation period determinations were known previously on this asteroid. Period analysis upon photometric observations carried out over five nights in 2021 August-September led an unequivocal rotation period of P = 2.5283 ± 0.0006 h associated with a bimodal lightcurve showing a rather large amplitude of 0.34 mag.

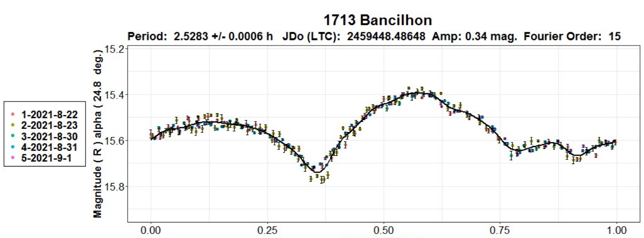

1727 Mette. A search of the LCDB database (Warner et al., 2009) finds multiple rotation period determinations on this Hungaria binary asteroid (Warner et al., 2013) over decades. Listed in chronological order, some of them are as follows: Wisniewski and McMillan (2.63 h, 1987), Prokof'eva et al. (2.637 h, 1992), Behrend (2.98125 h, 2006web), Gandolfi et al. (2.981 h, 2009), Warner et al. (2.98109 h, 2013), a sidereal value by Durech et al. (2.981174 h, 2020), Stephens and Warner (2.9804 h, 2020). Data from only two nights in late 2021 May obtained at SAO entirely cover the full rotational cycle corresponding to a period result of P = 2.982 ± 0.004 h found in the period analysis as the most favorable solution. This value matches many previously reported periods quite well.

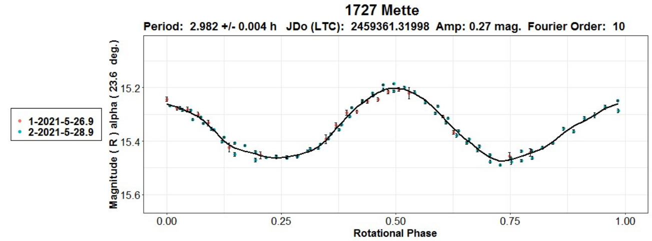

1949 Messina. A *BinAstPhot Survey* program target. An LCDB database search indicates several quite consistent previously determined results for rotation period: Pravec (3.6491 h, 2014web), Waszczak et al. (3.649 h and 3.635 h, 2015), and a sidereal value by Durech et al. (3.649308 h, 2016). Data taken on four nights in 2021 August confirm the previously derived results indicating a bimodal solution for a rotation period of P = 3.649 ± 0.002 h with associated lightcurve showing a quite large amplitude of 0.45 magnitudes.

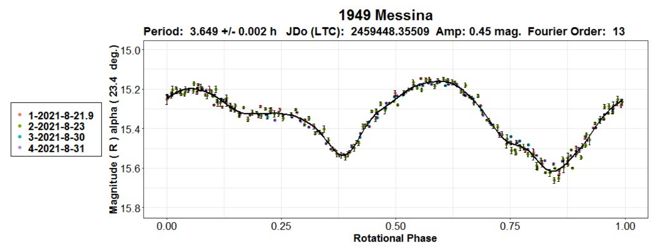

2044 Wirt. Another *BinAstPhot Survey* target and a confirmed Mars-crossing binary asteroid system. The companion was discovered photometrically by Donald Pray in 2006 within the *BinAstPhot Survey* (Pray et al., 2006). A number of fairly uniform rotation periods have been determined since 2005. For example, some of these are: Behrend (3.6900 h, 2005web), Pray et al. (3.6898 h, 2006), Waszczak et al. (3.690 h, 2015), Behrend (3.68989 h, 2016web). There are no satellite attenuation events in the SAO data collected in late February and early March 2021 over 3 nights only. Nevertheless, these data were sufficient to establish a secure rotation period result. A bimodal solution of P = 3.690 ± 0.003 h was found, which is in full accordance with the previously reported values.

2704 Julian Loewe. Recently processed backlog data on this spectroscopically confirmed V-type (Bus and Binzel, 2002) inner main-belt object obtained on three nights in 2020 September show a period of P = 2.641 ± 0.003 h, which is close to the value found by Oszkiewicz et al. (2.6385 h, 2020).

Number	Name	20yy/mm/dd	Phase	L_{PAB}	B_{PAB}	Period (h)	P.E.	Amp	A.E.	Grp
428	Monachia	21/03/24-20/03/28	23.5,24.0	127	6	3.635	0.003	0.37	0.03	MB-I
878	Mildred	21/08/16-21/09/10	*8.2,8.1	336	1	2.6607	0.0003	0.24	0.03	HER
894	Erda	21/04/23-21/04/25	16.8,16.9	143	-9	4.700	0.009	0.11	0.02	MB-O
1129	Neujmina	21/04/23-21/04/25	18.9,19.0	143	-8	5.06	0.02	0.11	0.03	EOS
1322	Coppernicus	21/06/21-21/06/28	29.1,28.1	316	25	4.352	0.003	0.16	0.02	MB-I
1671	Chaika	21/06/15-21/06/19	18.0,17.5	314	4	3.771	0.004	0.27	0.03	ASTR
1713	Bancilhon	21/08/21-21/09/01	24.8,20.6	8	-5	2.5283	0.0006	0.34	0.03	MB-I
1727	Mette	21/05/26-21/05/29	23.6,23.9	220	32	2.982	0.004	0.27	0.02	HUN
1949	Messina	21/08/21-21/08/31	23.4,19.5	4	7	3.649	0.002	0.45	0.03	MB-I
2044	Wirt	21/02/25-21/03/02	24.6,23.2	182	30	3.690	0.003	0.15	0.02	MC
2704	Julian Loewe	20/09/07-20/09/10	5.5,4.5	356	3	2.641	0.003	0.15	0.02	MB-I
2824	Franke	21/09/07-21/09/16	5.9,10.8	337	2	3.382	0.002	0.07	0.02	MB-I
2926	Caldeira	21/04/15-21/05/18	4.2,20.6	200	-1	6.651	0.002	0.15	0.03	FLOR
3760	Poutanen	21/06/07-21/07/04	17.2,24.2	232	11	2.9558	0.0003	0.19	0.02	MB-I
3807	Pagels	21/05/08-21/05/11	4.8,4.1	232	6	3.289	0.003	0.14	0.02	FLOR
3869	Norton	20/07/23-20/08/10	*6.9,5.3	312	6	7.605	0.003	0.14	0.01	MB-I
5235	Jean-Loup	21/06/23-21/07/13	19.0,9.8	303	4	2.4526	0.0003	0.11	0.02	MB-I
5402	Kejosmith	21/08/20-21/08/23	22.0,21.2	346	25	2.694	0.002	0.14	0.03	MB-I
5682	Beresford	21/06/03-21/06/15	4.5,9.0	251	7	3.774	0.002	0.08	0.03	MC
5972	Harryatkinson	21/06/20-21/07/14	*6.7,10.6	271	15	3.3889	0.0004	0.12	0.03	MB-M
6307	Maiztegui	21/06/26-21/07/14	8.2,14	260	10	5.290	0.002	0.27	0.03	MAR
6751	van Genderen	21/07/13-21/07/23	20.5,16.9	326	6	3.143	0.001	0.57	0.03	MB-I
7784	Watterson	21/06/13-21/06/21	16.0,17.9	261	24	5.080	0.003	0.12	0.02	MB-I
11452	1980 KE	21/08/03-21/08/07	13.7,12.3	327	11	3.128	0.003	0.16	0.02	MB-I
14427	1991 VJ2	21/08/09-22/08/15	7.1,5.5	323	7	6.250	0.007	0.25	0.03	MB-I
15317	1993 HW1	21/04/22-21/05/10	17.0,7.8	236	9	2.6580	0.0004	0.26	0.03	MB-I
15989	1998 XK39	21/04/06-21/04/30	*9.4,6.4	211	6	5.528	0.002	0.51	0.03	MB-I
19912	Aurapenenta	21/08/07-21/08/21	22.7,16.6	348	4	2.7826	0.0005	0.13	0.02	MB-I
140158	2001 SX169	21/06/02-21/06/02	73.4,45.7	289	11	3.143	0.002	0.62	0.05	NEA

Table I. Observing circumstances and results. Phase is the solar phase angle given at the start and end of the date range. If preceded by an asterisk, the phase angle reached an extrema during the period. LPAB and BPAB are the average phase angle bisector longitude and latitude. Grp is the asteroid family/group (Warner et al., 2009): EOS = Eos, FLOR = Flora, MB-I/M/O = main-belt inner /middle/ outer, MC = Mars Crosser, NEA = near-Earth asteroid, MAR = Maria, HER = Hertha, ASTR = Astraea, HUN = Hungaria.

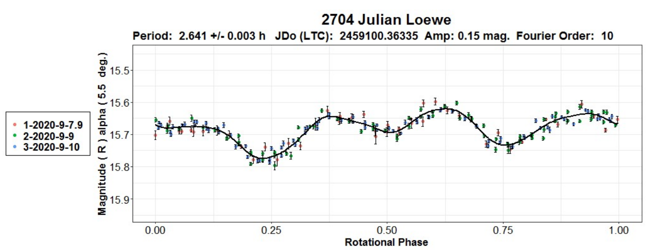

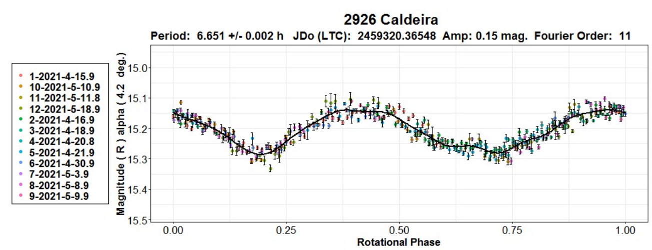

2824 Franke. Franco et al. (2015) found a value of 3.38 h for rotation period. The SAO data from 2021 September confirm this result yielding as secure result a period of P = 3.382 ± 0.002 h.

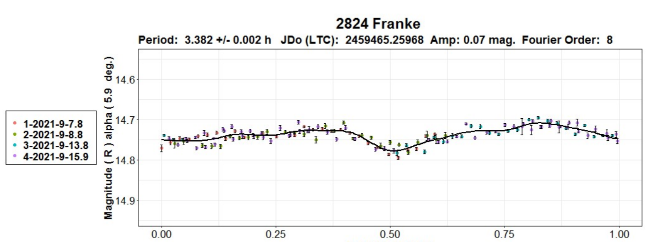

2926 Caldeira. The only prior rotation period result is the sidereal value reported more recently by Durech et al. (6.65099 h, 2020). A synodic period value obtained from the 2021 April-May SAO data is: P = 6.651 ± 0.002 h.

3760 Poutanen. A newly established rotation period result (P = 2.9558 ± 0.0003 h) from the SAO data taken in 2021 June-July is in good agreement with the previous results stated in the LCDB: Salvaggio et al. (2.956 h, 2017), Pal et al. (2.95588 h, 2020) and two previous ones found by Benishek (2.9554 h, 2018 and 2.957 h, 2021).

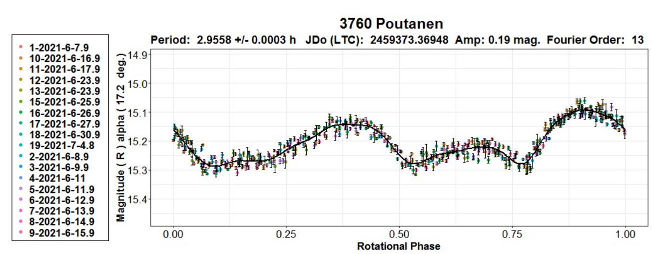

3807 Pagels.

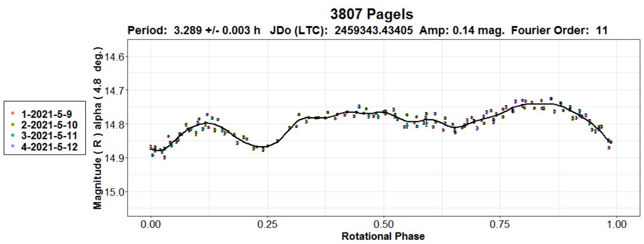

3869 Norton. Period analysis conducted over dense photometric data obtained at SAO in 2020 July-August over five nights implies a bimodal period solution of P = 7.605 ± 0.003 h as the most likely one. The only previous result from Pal et al. (17.0957 h, 2020) is in significant discrepancy with the result presented in this paper.

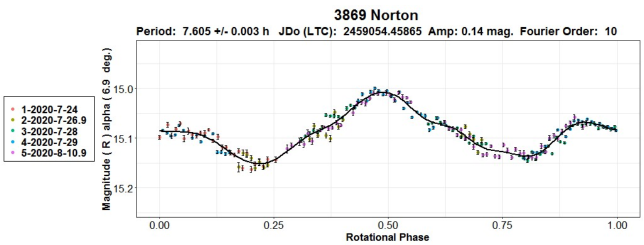

5235 Jean-Loup. Another V-type asteroid outside Vesta family. Oszkiewicz et al. (2020) found a period of 2.4524 h. The SAO data from 2021 June-July led to a virtually identical result: P = 2.4526 ± 0.0003 h.

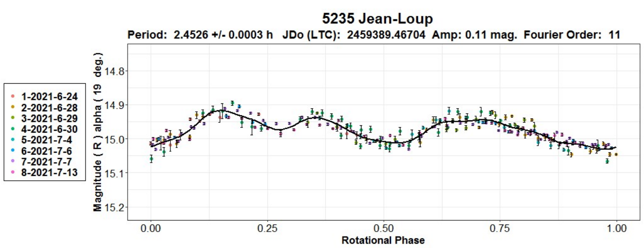

5402 Kejosmith. Benishek et al. (2018) photometrically detected a satellite around this inner main belt asteroid during its 2018 apparition. While a primary rotational period was established very well back then (2.69549 h), an ambiguity between the 16.31-hour and 32.62-hour satellite orbital period solutions remained to be resolved in the future. A new opportunity for photometric follow up of this binary taget emerged again in 2021 August. Due to increased volume of work on other binary asteroids within the *BinAstPhot Survey,* 5402 Kejosmith could have been observed to a limited extent and only on four bright Moon nights in the second half of August. Mutual events, which were very shallow in the 2018 apparition (0.03-0.07 mag.) were not observed this time. The cause of this could be somewhat increased noise due to the presence of the bright Moon in the sky, a quite limited amount of data obtained within relatively short observing runs, as well as the possibility that the system was outside the favorable mutual eclipse/occultation event geometry. Despite all the shortcomings of the newly obtained data, they served for a new rotation period determination, which resulted in a bimodal solution of P = 2.694 ± 0.002 h. This value is in full accordance with the 2018 apparition result.

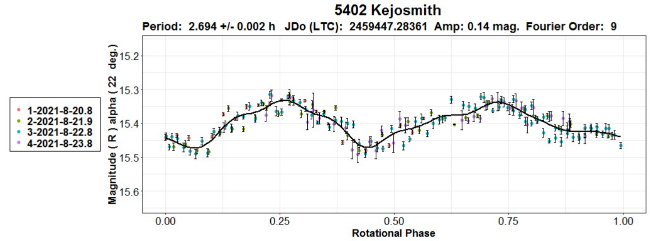

5682 Beresford. A rotation period result P = 3.774 ± 0.002 h found from the quite dense SAO data acquired on nine nights in 2021 June almost coincides with the result reported by Skiff (3.769 h, 2011web). Twice as much value was initially determined by Koff (7.536 h, 2005). Given the low lightcurve amplitude in the 2021 apparition of only 0.08 mag., there is still some uncertainty between the derived period P and twice the value 2P, which could be resolved by further photometric observations in future apparitions.

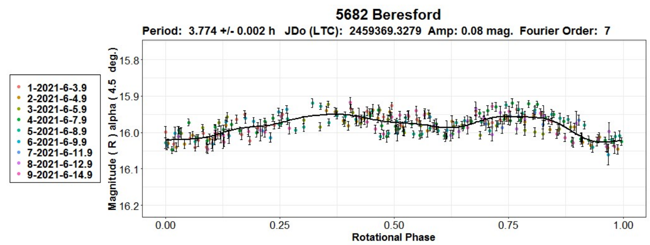

5972 Harryatkinson. Bonamico (3.376 h, 2020) and Pal et al. (3.38813 h, 2020) found fairly even period values. The result consistent with these values (P = 3.3889 ± 0.0004 h) was derived from dense photometric data obtained in 2021 June-July.

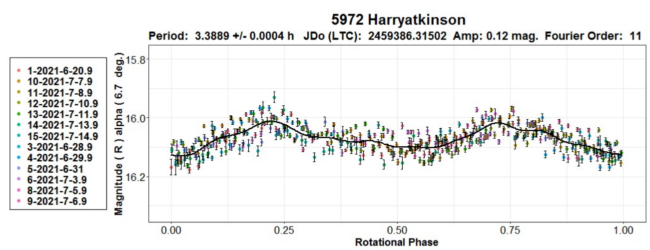

6307 Maiztegui.

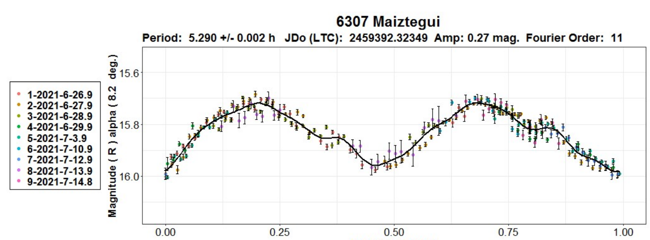

6751 van Genderen. The obtained period solution (P = 3.143 ± 0.001 h) is completely in line with almost all previously found results: Waszczak et al. (3.143 h, 2015), Pal et al. (3.14225 h, 2020) and a sidereal period by Durech et al. (3.142854 h, 2018).

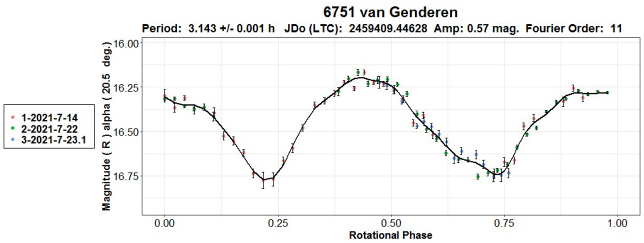

7784 Watterson. Skiff (2011) found a rotation period of 2.539 h. A dense combined photometric dataset was obtained on eight nights in 2021 June which show a value as twice as large as that found by Skiff, i.e. P = 5.080 ± 0.003 h. Lightcurve associated with this period shows four minima and four maxima per rotational cycle (a quadramodal solution) and a rather small amplitude of 0.12 mag. A split halves plot constructed for the 5.080-hour solution shows a clear difference between the two halves of the lightcurve, indicating its unambiguous plausibility over half the value.

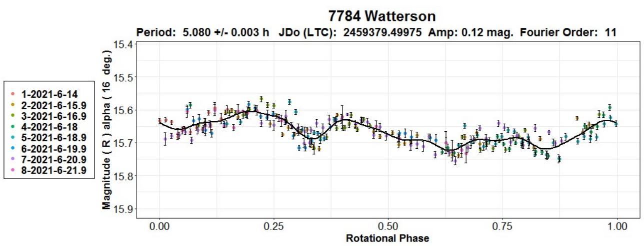

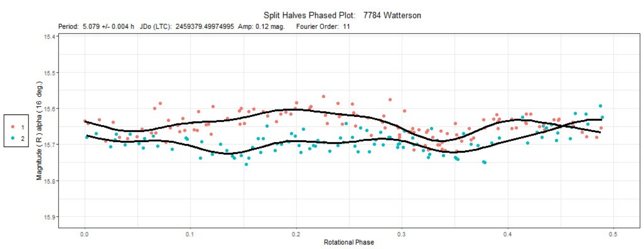

(11452) 1980 KE. Sparse photometry by Waszczak et al. (2015) shows a rotation period of 4.239 h, characterized as likely wrong in the LCDB (an uncertainty flag of U = 1). Period analysis of the combined dense photometry dataset obtained over four consecutive nights in 2021 August shows a different result as the most favorable solution: P = 3.128 ± 0.003 h.

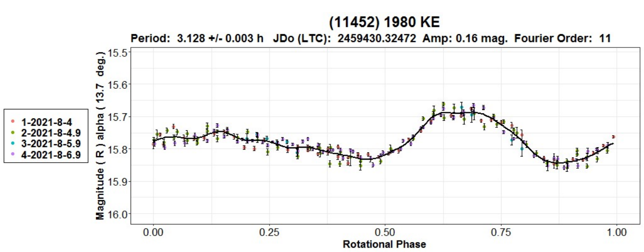

(14427) 191 VJ2. Five datasets obtained at SAO in 2021 August give an unmbiguous bimodal solution for period of P = 6.250 ± 0.007 h. Prior period result by Pal et al. (22.8637 h, 2020) turned out to be incorrect.

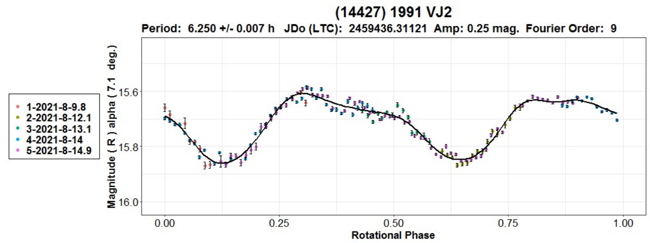

(15317) 1993 HW1. A *BinAstPhot Survey* inner main belt target. The found period (P = 2.6580 ± 0.0004 h) is fully consistent with other reported results: Pravec (2.6580 h, 2007web), Hawkins and Ditteon (2.660 h, 2008), Pal et al. (2.65804 h, 2020).

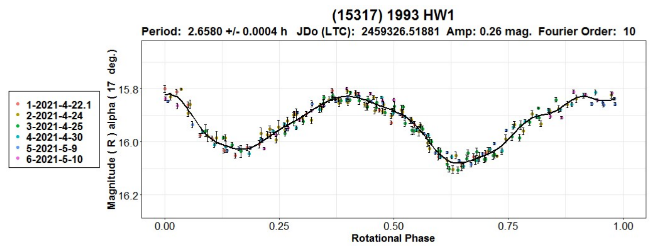

(15989) 1998 XK39. A *BinAstPhot Survey* inner main belt target with no prior rotation period results reported. Eight nights of observations in 2021 April at SAO resulted in a bimodal lightcurve phased to a period of P = 5.528 ± 0.002 h. Analyzing the same combined dataset Pravec finds a value of 5.52837 h (Pravec, 2021web).

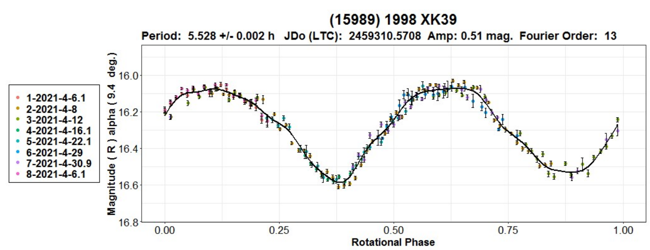

19912 Aurapenenta. Waszczak et al. (2015) derived a period of 2.340 h from sparse photometric dataset. Period analysis conducted over the dense SAO data obtained on nine nights in 2021 August shows a somewhat different bimodal period solution (P = 2.7826 ± 0.0005 h).

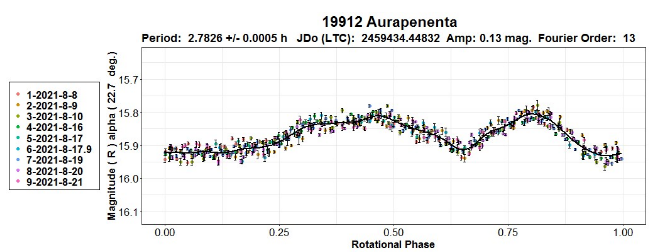

(140158) 2001 SX169. This NEA target was observed on seven nights in the first half of 2021 June. The found bimodal period solution of P = 3.143 ± 0.002 h fully fits the previously reported values by Vecchione et al. (3.1409 h, 2018) and Warner (3.1430 h, 2018b).

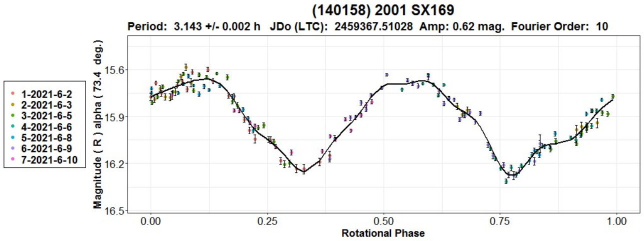

Acknowledgements

Observational work at Sopot Astronomical Observatory is supported by a 2018 Gene Shoemaker NEO Grant from The Planetary Society.

References

Behrend, R. (2001web, 2005web, 2006web, 2016web). Observatoire de Geneve web site. *http://obswww.unige.ch/~behrend/page_cou.html*

Benishek, V. (2018). "Lightcurve and Rotation Period Determinations for 29 Asteroids." *Minor Planet Bull.* **45**, 82-91.

Benishek, V.; Pravec, P.; Kucakova, H.; Hornoch, K.; Warner, B.; Oey, J.; Pilcher, F.; Chiorny, V. (2018). "(5402) Kejosmith." *CBET* **4561**.

Benishek, V. (2021). "Lightcurve and Rotation Period Determinations for 25 Asteroids." *Minor Planet Bull.* **48**, 280-285.

Bonamico, R. (2020). "Rotational Periods of Five Asteroids." *Minor Planet Bull.* **47**, 222-223.

Bus, S.J.; Binzel, R.P. (2002). "Phase II of the Small Main-Belt Asteroid Spectroscopic Survey. The Observations." *Icarus* **158**, 106-145.

Carbo, L.; Green, D.; Kragh, K.; Krotz, J.; Meiers, A.; Patino, B.; Pligge, Z.; Shaffer, N.; Getteon, R. (2009). "Asteroid Lightcurve Analysis at the Oakley Southern Sky Observatory: 2008 October thru 2009 March." *Minor Planet Bull*. **36**, 152-157.

Ditteon, R.; West, J. (2011). "Asteroid Lightcurve Analysis at the Oakley Southern Observatory: 2011 January thru April." *Minor Planet Bull.* **38**, 214-217.

Durech, J.; Hanuš, J.; Oszkiewicz, D.; Vančo, R. (2016). "Asteroid Models from the Lowell Photometric Database." *Astron. Astrophys.* **587**, A48.

Durech, J.; Hanus, J.; Ali-Lagoa, V. (2018). "Asteroid models reconstructed from the Lowell Photometric Database and WISE data." *Astron. Astrophys.* **617**, A57.

Durech, J.; Tonry, J.; Erasmus, N.; Denneau, L.; Heinze, A.N.; Flewelling, H.; Vanco, R. (2020). "Asteroid models reconstructed from ATLAS photometry." *Astron. Astrophys.* **643**, A59.

Fauerbach, M.; Brown, A. (2018). "Lightcurve Analysis of Minor Planets 1132 Hollandia, 1184 Gaea, 1322 Coppernicus, 1551 Argelander, and 3230 Vampilov." *Minor Planet Bull.* **45**, 240-241.

Franco, L.; Marchini, A.; Papini, R. (2015). "Lightcurve Analysis for 2824 Franke and 3883 Verbano." *Minor Planet Bull.* **42**, 114.

Gandolfi, D.; Cigna, M.; Fulvio, D.; Blanco, C. (2009). "CCD and Photon-Counting Photometric Observations of Asteroids Carried Out at Padova and Catania Observatories." *Planetary and Space Science* **57**, 1-9.

Hawkins, S.; Ditteon, R. (2008). "Asteroid Lightcurve Analysis at the Oakley Observatory - May 2007." *Minor Planet Bull.* **35**, 1-4.

Higgins, D.; Goncalves, R.M.D. (2007). "Asteroid Lightcurve Analysis at Hunters Hill Observatory and Collaborating Stations – June - September 2006." *Minor Planet Bull.* **34**, 16-18.

Koff, R.A. (2005). "Lightcurve Photometry of Asteroids 212 Medea, 517 Edith, 3581 Alvarez, 5682 Beresford, and 5817 Robertfrazer." *Minor Planet Bull.* **32**, 32-34.

Menke, J.; Cooney, W.; Gross, J.; Terrell, D.; Higgins, D. (2008). "Asteroid Lightcurve Analysis at Menke Observatory." *Minor Planet Bull.* **35**, 155-160.

Noschese, A.; Vecchione, A.; Ruocco, N.; Izzo, L. (2018). "Lightcurve Analysis for Minor Planets 1322 Coppernicus and 9148 Boriszaitsev." *Minor Planet Bull.* **45**, 70-71.

Oszkiewicz, D.; Troianskyi, V.; Föhring, D.; Galád, A.; Kwiatkowski, T.; Marciniak, A.; Skiff, B.A.; Geier, S.; Borczyk, W.; Moskovitz, N.A.; Kankiewicz, P.; Gajdoš, Š.; Világi, J.; Polčic, L.; Kluwak, T. and 5 colleagues. (2020). "Spin Rates of V-type Asteroids." *Astron. Astrophys.* **643**, A117.

Pal, A.; Szakáts, R.; Kiss, C.; Bódi, A.; Bognár, Z.; Kalup, C.; Kiss, L.L.; Marton, G.; Molnár, L.; Plachy, E.; Sárneczky, K.; Szabó, G.M.; Szabó, R. (2020). "Solar System Objects Observed with TESS - First Data Release: Bright Main-belt and Trojan Asteroids from the Southern Survey." *Ap. J. Supl. Ser*. **247**, 26-34.

Pravec, P. (2007web, 2014web, 2021web). Photometric Survey for Asynchronous Binary Asteroids web site. *http://www.asu.cas.cz/~ppravec/newres.txt*

Pray, D.; Pravec P.; Kusnirak, P.; Cooney, W.; Gross, J.; Terrell, D.; Galad, A.; Gajdos, S.; Vilagi, J.; Durkee, R. (2006). "(2044) Wirt." *CBET* **353**.

Prokof'eva, V.V.; Demchik, M.I.; Golub', A.I. (1992). "TV Photometry of Asteroids: Brightness Curve of Asteroid 1727 Mette." *Solar System Research* **26**, 373-375.

R Core Team (2020). R: A language and environment for statistical computing. R Foundation for Statistical Computing.Vienna, Austria. *https://www.R-project.org/*

Salvaggio, F; Marchini, A.; Papini, R. (2017). "Rotation Period Determination for 3760 Poutanen and 14309 Defoy." *Minor Planet Bull.* **44**, 354-355.

Skiff, B.A. (2011web). Posting on CALL web site. *https://minplanobs.org/MPInfo/php/call.php*

Stephens, R.D. (2002). "Photometry of 866 Fatme, 894 Erda, 1108 Demeter, and 3443 Letsungdao." *Minor Planet Bull.* **29**, 2-3.

Stephens, R.D.; French, L.M. (2011). "878 Mildred Revealed." *Minor Planet Bull.* **38**, 1-2.

Stephens, R.D.; Warner, B.D. (2020). "Main-belt Asteroids Observed from CS3: 2019 July to September." *Minor Planet Bull.* **47**, 50-60.

Vecchione, A.; Noschese, A.; Catapano, A. (2018). "Lightcurve Analysis and Rotation Period for (140158) 2001 SX169." *Minor Planet Bull.* **45**, 183-184.

VizieR (2021). *http://vizier.u-strasbg.fr/viz-bin/VizieR*

Warner, B.D.; Harris, A.W.; Pravec, P. (2009). "The Asteroid Lightcurve Database." *Icarus* **202**, 134-146. Updated 2021 June. *http://www.minorplanet.info/lightcurvedatabase.html*

Warner, B.D. (2012). The MPO Users Guide: A Companion Guide to the MPO Canopus/PhotoRed Reference Manuals. BDW Publishing, Colorado Springs, CO.

Warner, B.D.; Stephens, R.D.; Harris, A.W. (2013). "(1727) Mette." *CBET* **3402**.

Warner, B.D. (2014). "Asteroid Lightcurve Analysis at CS3-Palmer Divide Station: 2014 January-March." *Minor Planet Bull.* **41**, 144-155.

Warner, B.D. (2018a). MPO Canopus software, version 10.7.11.3. *http://www.bdwpublishing.com*

Warner, B.D. (2018b). "Near-Earth Asteroid Lightcurve Analysis at CS3-Palmer Divide Station: 2017 October-December." *Minor Planet Bull.* **45**, 138-147.

Waszczak, A.; Chang, C.-K.; Ofek, E.O.; Laher, R.; Masci, F.; Levitan, D.; Surace, J.; Cheng, Y.-C.; Ip, W.-H.; Kinoshita, D.; Helou, G.; Prince, T.A.; Kulkarni, S. (2015). "Asteroid Light Curves from the Palomar Transient Factory Survey: Rotation Periods and Phase Functions from Sparse Photometry." *Astron. J.* **150**, A75.

Wisniewski, W.Z.; McMillan, R.S. (1987). "Differential CCD Photometry of Faint Asteroids in Crowded Star Fields and Nonphotometric Sky Conditions." *Astron. J.* **93**, 1264.

Wisniewski, W.Z.; Michalowski, T.M.; Harris, A.W.; McMillan, R.S. (1997). "Photometric Observations of 125 Asteroids." *Icarus* **126**, 395-449.

LIGHTCURVES OF SEVEN ASTEROIDS

Eric V. Dose
3167 San Mateo Blvd NE #329
Albuquerque, NM 87110
mp@ericdose.com

(Received: 2021 October 13)

We present lightcurves, synodic rotation periods, and G value (H-G) estimates for seven asteroids.

We present asteroid lightcurve photometry results obtained by following the workflow process described by Dose (2020a), with later improvements (Dose, 2020b). This workflow applies to each image an ensemble of typically 20-60 nearby ATLAS refcat2 catalog (Tonry et al, 2018) comparison ("comp") stars as a basis for asteroid photometry. Diagnostic plots and numerous comp stars allow for effective identification and removal of outlier, variable, and poorly measured comp stars.

The custom workflow produces a time series of asteroid magnitude estimates on Sloan r' (SR) catalog basis, unreduced and without H-G adjustment. These magnitudes are imported directly into *MPO Canopus* software (Warner, 2018, version 10.8.4.11) where they are adjusted for distances and phase-angle dependence, fit by Fourier analysis including identifying and ruling out of aliases, and plotted. Phase-angle dependence is corrected with a H-G model, using the *G* value that minimizes fit RMS error across all nights' data.

No nightly zero-point adjustments (DeltaComps in *MPO Canopus* terminology) were made to any session herein, other than by adjusting the G value (H-G phase model). All lightcurve data herein have been submitted to ALCDEF.

Lightcurve Results

Seven asteroids were observed from Deep Sky West observatory (IAU V28) at 2210 meters elevation in northern New Mexico. Images were acquired with a 0.35-meter SCT reduced to f/7.7; a SBIG STXL-6303E camera cooled to -35 C and fitted with a Clear filter (Astrodon); and a PlaneWave L-500 mount. The equipment was operated remotely via ACP software (DC-3 Dreams, version 8.3), running plan files generated for each night by the author's python scripts (Dose, 2020a). Observations often cycled among 2-4 asteroids. Exposure times targeted 5-8 millimagnitudes uncertainty in asteroid instrumental magnitude, subject to a minimum of 120 seconds to ensure suitable comp-star photometry, and to a maximum of 900 seconds. All exposures were autoguided.

FITS images were plate-solved by *PinPoint* (DC-3 Dreams) or *TheSkyX* (Software Bisque) and were calibrated using temperature-matched, median-averaged dark images and recent flat images of a flux-adjustable flat panel. Every photometric image was visually inspected; all images with poor tracking, obvious interference by cloud or moon, or having stars or other light sources within 10 arcseconds of the target asteroid were excluded. Photometry-ready images that pass these screens were submitted to the workflow, which applies separately measured second-order transforms from Clear filter to deliver asteroid magnitudes in Sloan r' passband.

In this work, "period" refers to an asteroid's synodic rotation period, and "SR" denotes the Sloan r' passband.